Towards a Multivariate Probabilistic Morphology for Colour Images

Mihai IVANOVICI, Alexandru CĂLIMAN; MIV Imaging Venture Laboratory, Department of Electronics and Computers, Faculty of Electrical Engineering and Computer Science, "Transilvania" University; Braşov, România

Noël RICHARD, Christine FERNANDEZ-MALOIGNE; XLIM-SIC UMR CNRS 6172, Signals, Images and Communications, University of Poitiers; Poitiers, France

Abstract

The mathematical morphology for colour images faces the delicate issue of defining a total order in a vectorial space. There are various approaches based on partial or total orders defined for color images. We propose a probabilistic approach, that uses principal component analysis (PCA), for the computation of the convergence colours, i.e. the extrema of a set. Then we define two pseudo-morphological operations, the dilation and the erosion, applying the Chebyshev's inequality on the first eigenvector of the image colour data. As an application, we use our approach to extract the Beucher colour gradient. We discuss the advantages and disadvantages of our approach, we comment our results and then we conclude this paper.

Introduction

The classical morphology was defined for binary objects. The extension of the morphology from binary to gray-scale by Serra [16], Sternberg [17] and Haralick [6] introduced a natural morphological generalization of the dilation and erosion, the two fundamental morphological operations. However, the approaches are limited to the gray-scale domain and their extension to the colour domain is not straightforward.

There exist several approaches for colour images [8] [10] [9], which are based on total ordering in the three-dimensional colour space. Some of them, are defined in HLS [11] [7] [2] or similar perceptual colour spaces, and the defined order strongly depends on the choice of H_0 - the hue origin. Therefore, for the approaches that use a lexicographical order, the convergence points, i.e. the minimum and the maximum of the set of points in the entire image, are basically specified in the process of defining the priority of the colour planes. In addition, for several approaches, like [14] for instance, the dilation and erosion converge towards white and black, respectively, i.e. the "natural" extrema of the colour space. A generalized total order in a colour space has been proposed by J. Angulo in [1], but this still does not solve a fundamental problem: the order is not "natural" - red shades are *larger* than green shades, and further on, according to the defined order, other red shades are *smaller* than the same green ones (see Figure 1(c), where Δ_2 should be smaller than Δ_1 from the human perception point of view, which is not the case when ordering based on priority per component is used) and this kind of approaches leads to non-linearity from a human perception point of view.

Recently, there has been an attempt of using probability density functions in order to define the morphological operations for colour images [18], where the statistical depth functions are used for establishing an order between the colours. Other recent approaches are based on fuzzy logic [5] and a great interest has also been shown on adaptive morphology [3].

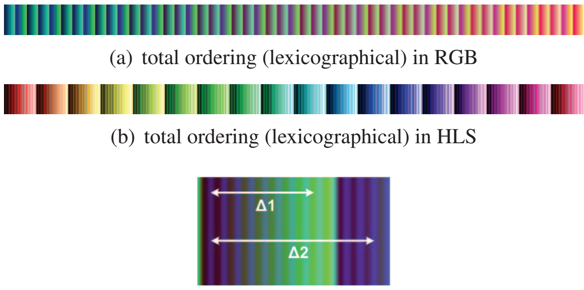

(a) total ordering (lexicographical) in RGB

(b) total ordering (lexicographical) in HLS

(c) detail of (a)

Figure 1. *Colour total ordering in RGB and HLS with priority defined per channel.*

A multivariate probabilistic approach

The Minkowski definition of the erosion and dilation relies on the computation of the maximum and the minimum values of a set. Therefore the key element of the classic morphology is the computation of the extrema of a given set [16]. What we propose is to construct the maximum and the minimum values in a probabilistic manner. Some probabilistic approaches already exist by Haralick[6] and Ivanovici [12], but they are either for binary signals or they are restricted to a marginal analysis. The work of Barnett [4] has to be also mentioned, as it defines a generic framework for the ordering of multivariate data.

Our approach first determines two convergence colours which will constitute the global maximum and minimum of the set of colours for a given image. The two extrema are computed according to the following algorithm:

1. compute the 3D histogram in the RGB color space
2. apply PCA in order to determine the principal vectors of the multivariate colour data
3. apply Chebyshev inequality on the first eigenvector (the one corresponding to the largest eigenvalue) in order to establish the two extrema
4. choose the *maximum* colour as the one with the largest energy (the *minimum* colour will be the other one);

The Chebyshev inequality [13] states that for a positive random variable ξ with expected value $\overline{\xi}$ and standard deviation σ_ξ we can write: $P\{|\xi - \overline{\xi}| \geq k\sigma_\xi\} \leq \frac{1}{k^2}$.

This offers us the possibility of constructing the extrema of a given set, based on the mean and the standard deviation. In our case, the random variable is represented through the projection of the points on the first eigenvector and, consequently, the two extrema ($\mathcal{E}_1$ and $\mathcal{E}_2$) may be computed along this eigenvector as:

$$\begin{cases} \mathcal{E}_1\{\xi\} & \stackrel{\text{def}}{=} \overline{\xi} + k\sigma_\xi, \\ \mathcal{E}_2\{\xi\} & \stackrel{\text{def}}{=} \overline{\xi} - k\sigma_\xi \end{cases} \tag{1}$$

The computation along the first eigenvector is done by rotating the entire set of points around the mean point, as required by the PCA, so that the first eigenvector is identical with the X axis of the original space. In Figure 2 the 2D case is depicted, showing the rotation and the construction of the extreme points for a set of random points of zero mean. We computed k automatically, as the largest possible value so that both global extreme points fall inside the RGB cube. At the limit, it is accepted that one of the global extreme points to be on the surface of the RGB cube and the other one inside. In this way we make sure that the resulting colours remain inside the RGB colour cube and still can be rendered for visualization. A large value of k may lead to extrema which are outside the gamut and therefore cannot be rendered. In order to choose the maximum and the minimum between the two extrema, we investigate the energy of the two values, expressed as the volume given by the multiplication of the 3 colour components, $V(\mathcal{E}) = r_{\mathcal{E}} \times g_{\mathcal{E}} \times b_{\mathcal{E}}$, or defined as the sum of the squares of the three components, $V(\mathcal{E}) = r_{\mathcal{E}}^2 + g_{\mathcal{E}}^2 + b_{\mathcal{E}}^2$, which may be used if the first definition leads to equality between the two points.

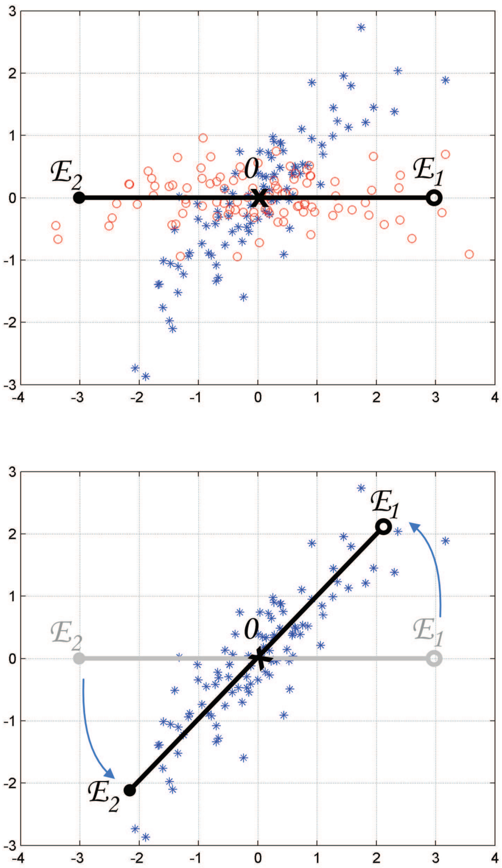

Figure 2. Rotation of the original set of points (blue stars) so that the first eigenvector to be identical with the X axis of the space (red circles). Extrema $\mathcal{E}_1$ and $\mathcal{E}_2$ computation along the principal eigenvector using equation (1).

Once the convergence colours are determined, the local minimum and maximum (in the neighborhood of size ε in case of a flat structuring element) are computed in the following way:

1. compute two local extreme points e_1 and e_2 similarly with the global extrema $\mathcal{E}_1$ and $\mathcal{E}_2$;
2. calculate the projection of the two local extrema on the line determined by the global minimum and maximum (the direction given by the first eigenvector of the entire image, see Figure 3);
3. translate the two projections so that their mean to be the same as the global extrema mean; the translation is performed in order to avoid situations in which both local extrema projections are outside the segment determined by the global extrema, both on the same side of one extremum (in this case, if we simply consider the distances to the global extrema, the local minimum and maximum would be swapped);
4. the local extrema corresponding to the point which after projection and translation is the closest to the global maximum will be the local maximum; the other one will be the local minimum;
5. if the two projections are equal (i.e. the local and global first eigenvectors are orthogonal), the local extrema are computed in the same way but using the second eigenvector of the local data; if again, the two projections of the local date are equal we consider the third eigenvalue for constructing the extrema—but in our experiments we haven't encountered these situations.

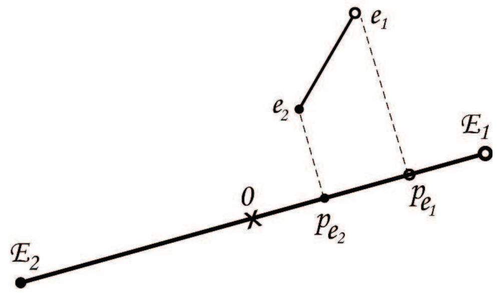

(a) "inside"

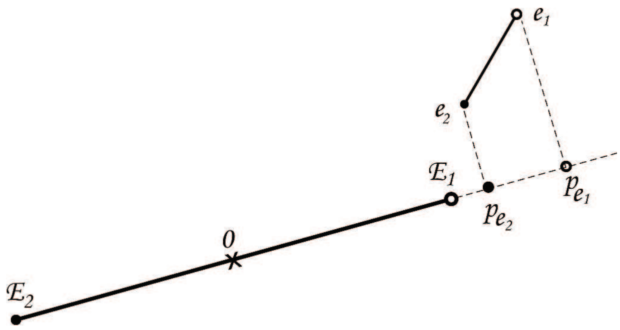

(b) "outside"

Figure 3. Possible orientations of local extrema with respect to global extrema. $\mathcal{P}_{e_1}$ and $\mathcal{P}_{e_1}$ are the projections of local extrema on the direction given by the global extrema

For our approach we used the RGB colour space and the distance for the local extrema computation was Euclidian, defined for two colours $\mathcal{C}_1 = (r_1, g_1, b_1)$ and $\mathcal{C}_2 = (r_2, g_2, b_2)$ as $d(\mathcal{C}_1, \mathcal{C}_2) = \sqrt{(r_1 - r_2)^2 + (g_1 - g_2)^2 + (b_1 - b_2)^2}$.

Results

As we already pointed out, there exist several approaches for colour morphology and the difficulty lies in the choice of the "good" one. Classically, morphological operators are combined to produce non-linear filters, but how could one validate one approach by just subjectively assess the result from a visual point of view? In order to prove the usefulness of our approach we present also the results of a gradient extraction application based on the Beucher's expression [15] of a symmetrical gradient.

We use the images in Figure 4 for testing our method.

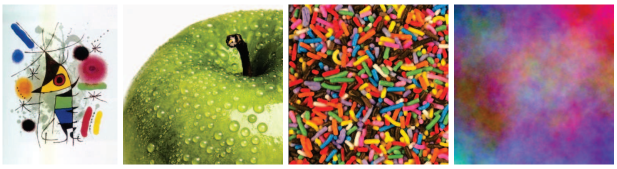

(a) *Miro* (b) *apple* (c) *candies* (d) *fractal*

Figure 4. *Original colour test images.*

We present a first set of results in Figures 5 and 6 for different sizes ε of the structuring element.

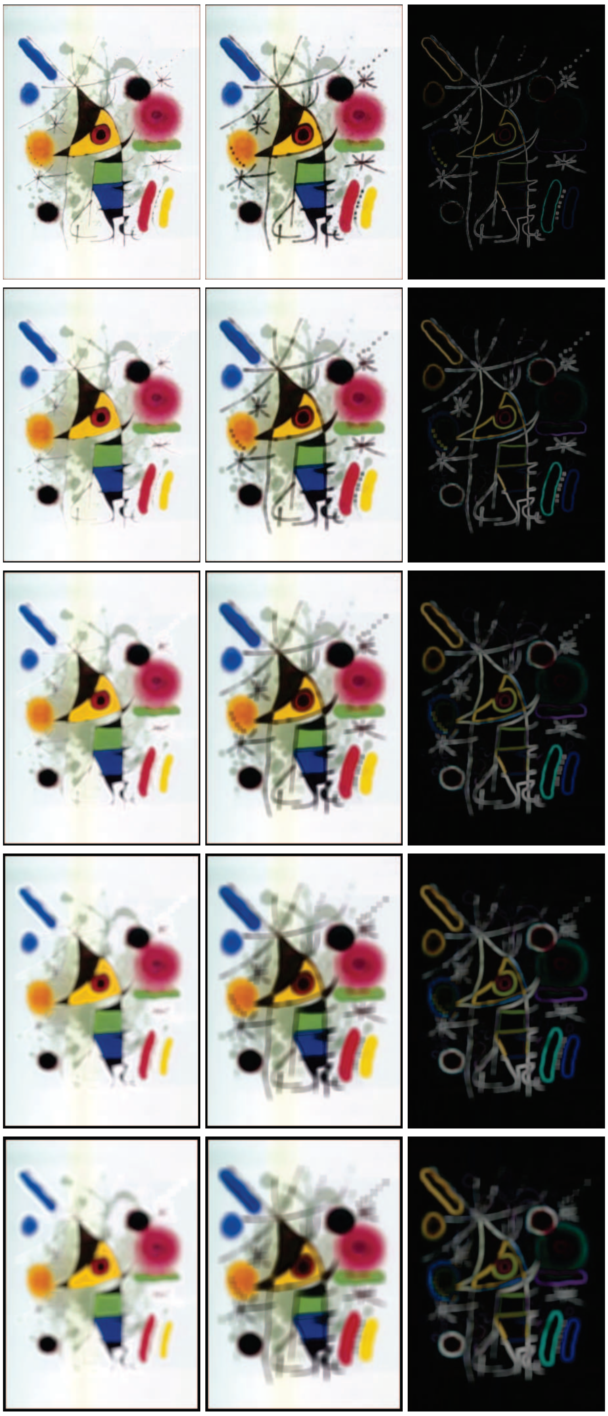

Figure 5. *Dilations (first column), erosions (second column) and Beucher gradients (third column) for various structuring element sizes ($\varepsilon = 3,5,7,9$ & 11) for the "singer" painting by Miro.*

As one would expect, the convergence point for the dilation of *"Miro"* image is practically white = (250, 255, 251), but the convergence point for the erosion, given by the PCA approach is not black = (163, 153, 146). This is the reason why the black regions in the image are lightened after erosion. Another important remark is that both the dilations and erosions became blurrier than the original image, similar to the effect of a low-pass filter.

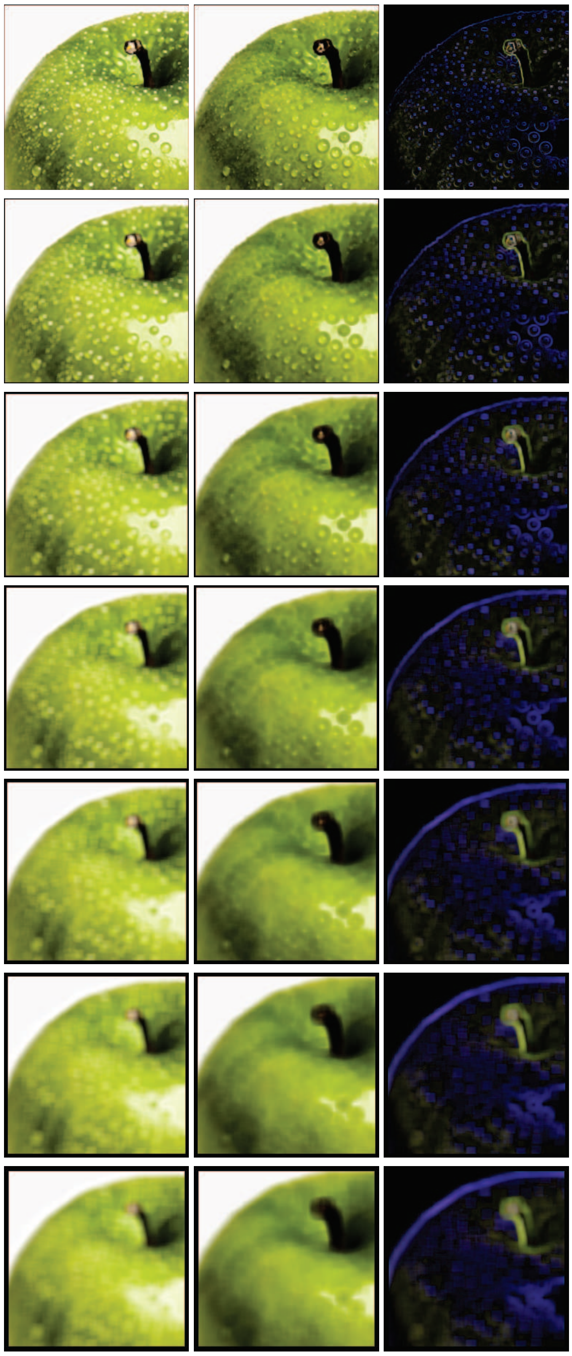

Figure 6. *Dilations (first column), erosions (second column) and Beucher gradients (third column) for various structuring element sizes ($\varepsilon = 3,5,7,9,11,13$ & 15) for the "apple" image.*

This happens because the PCA is computed relative to the mean of each local set of points and that mean does not change dramatically between two consecutive local sets. The convergence points for the *"apple"* image are = (207, 215, 142) for dilation and = (72, 81, 0) for erosion. It can be seen that the apple stalk is favored by the erosion operation being emphasized by it, while the dilation tend to lighten the whole object. This is in fact only a visual perception because the dilation and the erosion operations move all the colours in the image towards the maximum and respectively the minimum global points. Also notice the disappearance of the specularity of the water drops, which is a desired effect of the morphological erosion, i.e. the removal of small objects, smaller than the structuring element size.

Another set of results is presented in Figures 8 and 9. In this case the morphological operations are applied to colour textured image. For the candies image, the convergence points are = (255, 167, 102) for dilation and = (44, 26, 23) for erosion while for the fractal image the global maximum is = (88, 131, 255), and the global minimum is = (205, 57, 30). On these results one may notice some discontinuity regions. These discontinuities appear due to the fact that the projections of the local extreme points, in the local minimum and maximum computation, change their order relative to the global extrema while sweeping the structuring element onto the image (the phenomenon is illustrated in Figure 7). The discontinuities are more obvious in textured images where the texture is uniform but colour is not, thus the erosion and dilation based on the colour distribution are also discontinuous.

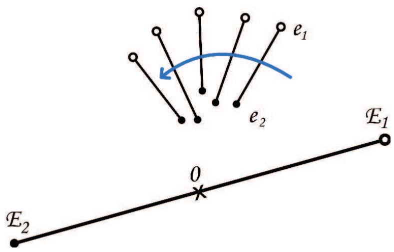

Figure 7. Evolution of the relative orientation of the local extrema with respect to global extrema, causing discontinuities.

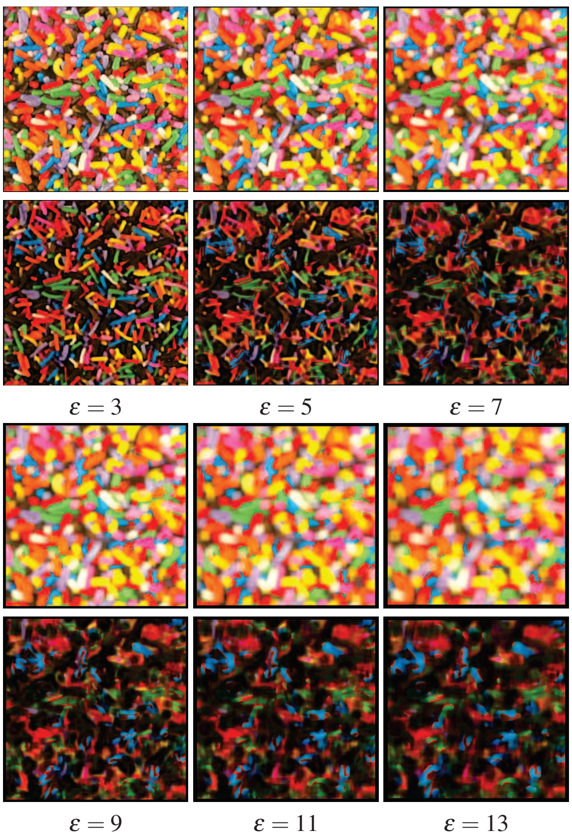

Figure 8. Dilations (1^{st} and 3^{rd} rows) and erosions (2^{nd} and 4^{th} rows) for various structuring element sizes for "candies".

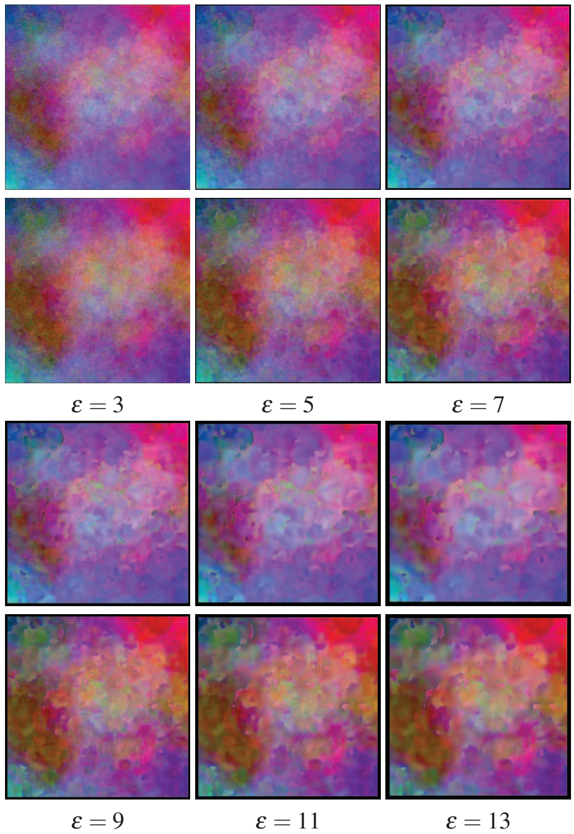

Figure 9. Dilations (1^{st} and 3^{rd} rows) and erosions (2^{nd} and 4^{th} rows) for various structuring element sizes for "fractal".

Duality

In this section we prove both mathematically and experimentally the duality property of our pseudo-morphological operators. Mathematically, in any local neighborhood of size ε, because the distances between the mean of the colour points O and the two extrema are equal, $d(O,\mathcal{E}_1) = d(O,\mathcal{E}_2) = k\sigma_\xi$, this implies that one extremum is the complement of the other, with respect to the origin O, therefore $\mathcal{E}_1 = \overline{\mathcal{E}_2} = -\mathcal{E}_2$ and vice-versa.

In Figure 10 we present the dilation of the *"Miro"* image with a structuring element of size 11 (a), the negative of the original image (b), the erosion of this image with the same structuring element size (c) and the negative of the erosion (d), which is equal to the dilation of the original image. The difference image (e) is completely black, except for two pixels for which there is an absolute difference of 1 for one of the colour components, most likely as a consequence of type conversions and rotations. The black border due to the size of the structuring element affecting image (a) was disregarded.

Conclusions

We propose a multivariate probabilistic way to chose the convergence colours for morphological operations. We define a pseudo-dilation and a pseudo-erosion for colour images based on the principal component analysis combined with the Chebyshev inequality with respect to the convergence colours statistically chosen. The key element of our approach is the definition of the extrema of a given set, chosen along the first eigenvector direction for a cloud of colours.

Despite the fact that the RGB is not a perceptual colour space, the three colour components are highly correlated which is appropriate for the use of the PCA in order to determine the trend

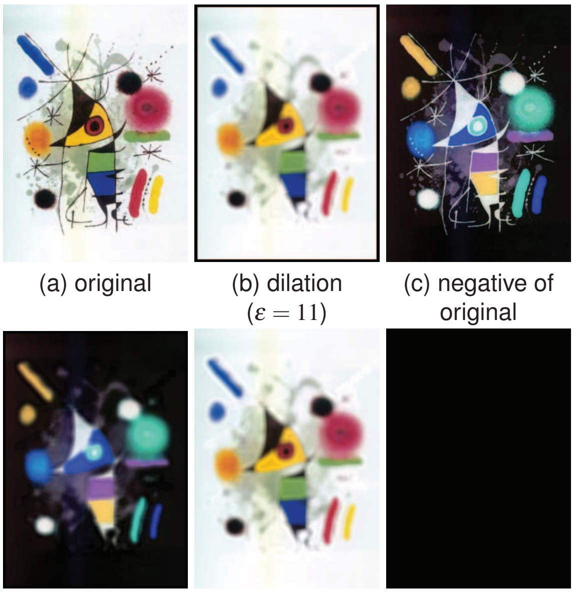

(a) original (b) dilation ($\varepsilon = 11$) (c) negative of original

(d) erosion of (c) ($\varepsilon = 11$) (e) negative of (d) (f) difference of (b) and (e)

Figure 10. *Experimental proof of the duality property.*

of the colours in the image.

We presented our results for both object images and texture images. We prove the duality of the two pseudo-morphological operators and we show that our approach can be successfully used to compute a colour gradient, thus proving both the usefulness and the validity of our approach. We conclude that our approach may represent an alternative for the choice of the convergence colours or for the choice of the hue origin as opposed to an arbitrary specification. The disadvantages of our method would be that for textured images some discontinuities appear in the results and that the results do not preserve the original colours by creating new colours. In our future work we consider using the CIELab colour space instead of RGB due to the fact that the Euclidian norm, which we use, introduces nonlinearities in the RGB colour space.

Acknowledgments

This paper is partially supported by the Sectoral Operational Programme for Human Resources Development (SOP HRD), ID76945 financed from the European Social Fund and by the Romanian Government.

References

[1] J. Angulo. Geometric algebra colour image representations and derived total orderings for morphological operators - part i: Colour quaternions. *Visual Communication and Image Representation*, 2009.

[2] J. Angulo and G. Flandrin. Microscopic image analysis using mathematical morphology: Application to haematological cytology. In *Science, Technology and Education of Microscopy: An overview*, volume 1, pages 304–312. FORMATEX Eds., Badajoz, Spain, 2003.

[3] Jesus Angulo. Morphological bilateral filtering and spatially-variant adaptive structuring functions. In Pierre Soille, Martino Pesaresi, and Georgios Ouzounis, editors, *Mathematical Morphology and Its Applications to Image and Signal Processing*, volume 6671 of *Lecture Notes in Computer Science*, pages 212–223. Springer Berlin / Heidelberg, 2011.

[4] V. Barnett. The ordering of multivariate data. *Journal of the Royal Statistical Society A*, 139(3):318–354, 1976.

[5] Isabelle Bloch. Fuzzy bipolar mathematical morphology: A general algebraic setting. In Pierre Soille, Martino Pesaresi, and Georgios Ouzounis, editors, *Mathematical Morphology and Its Applications to Image and Signal Processing*, volume 6671 of *Lecture Notes in Computer Science*, pages 13–24. Springer Berlin / Heidelberg, 2011.

[6] Haralick Dougherty Ha, E. Dougherty, J. Ha, T. Kanungo, S. Karasu, C. K. Lee, L. Rystrom, V. Ramesh, and I. Phillips. Statistical morphology. In *In Proceedings of the First International Conference on Computer Vision*, pages 516–520, 1987.

[7] A. Hanbury. The taming of the hue, saturation and brightness colour space. In *7th Computer Vision Winter Workshop*, pages 234–243, Bad Aussee, Austria, 2002.

[8] A. Hanbury. Constructing cylindrical coordinate colour spaces. *Pattern Recognition Letters*, 29(4):494–500, 2008.

[9] A. Hanbury and J. Serra. Mathematical morphology in the hls colour space. In *12th British Machine Vision Conference*, pages 451–460, Manchester, UK, 2001.

[10] A. Hanbury and J. Serra. Morphological operators on the unit circle. *IEEE Transactions on Image Processing*, 10(12):1842–1850, 2001.

[11] A. Hanbury and J. Serra. Mathematical morphology in the cielab space. *Image Analysis and Stereology*, 21(3):201–206, 2002.

[12] M. Ivanovici and N. Richard. Colour covering blanket. In *International Conference on Image Processing, Computer Vision and Pattern Recognition*, Las Vegas, Nevada, USA, July 12-15 2010.

[13] D. McDonald. *Elements of Applied Probability for Engineering, Mathematics and System Science*. World Scientific Publishing, 2004.

[14] Noël Richard, Anne-Sophie Capelle Laizé, and C. Fernandez Maloigne. Colour morphology with perceptual behaviour and vectorial structuring element. In *11th Congress of the International Colour Association (AIC) 2009 11th Congress of the International Colour Association (AIC) 2009*, Sydney Australie, 2009.

[15] J.F. Rivest, P. Soille, and S. Beucher. Morphological gradients. In Editors Edward R. Dougherty; Jaakko T. Astola; Charles G. Boncelet, Jr., editor, *SPIE - Non Linear Processing III*, pages 139–150. SPIE, April 1992.

[16] J. Serra. *Image Analysis and Mathematical Morphology*, volume I. Academic Press, 1982.

[17] S.R. Sternberg. Grayscale morphology. *Computer Vision, Graphics, and Image Processing*, 35(3):333–355, 1986.

[18] Santiago Velasco-Forero and Jesus Angulo. Mathematical morphology for vector images using statistical depth. In Pierre Soille, Martino Pesaresi, and Georgios Ouzounis, editors, *Mathematical Morphology and Its Applications to Image and Signal Processing*, volume 6671 of *Lecture Notes in Computer Science*, pages 355–366. Springer Berlin / Heidelberg, 2011.